# Sensitivity Analysis of Process Parameters in Laser Deposition

Zhiqiang Fan, Kaushik Phatak and Frank Liou
Department of Mechanical and Aerospace Engineering, University Of Missouri–Rolla
1870 Miner Circle, Rolla, MO 65409
573-341-4603, liou@umr.edu
Reviewed, accepted August 30, 2005

**Abstract:** In laser cladding with powder injection process, process output parameters, including melt pool temperature and melt pool dimensions, are critical for part quality. This paper uses simulation and experiments to investigate the effect of the process input parameters: laser power, powder mass flow rate, and scanning speed on the output parameters. Numerical simulations and experiments are conducted using a factorial design. The results are statistically analyzed to determine the significant factors and their interactions. The simulation results are compared to experimental results. The quantitative agreement/disagreement is discussed and further research is outlined.

## 1. Introduction

Laser Metal Deposition (LMD) is a layered deposition process where a laser melts metal powder to form a melt pool, which quickly solidifies and forms a track. This process can produce parts requiring high accuracy and flexibility. It can be used to create functional prototypes and functional gradient material (FGM) metal parts. Also, parts may be repaired using the LMD process, thus, reducing scrap and extending product service life [1]. The advantage of this process is that, complex geometries can be constructed with high degrees of accuracy to achieve near net shape with a solid model of the part [2].

One of the subjects in this field is melt pool thermal behavior. Due to the highly localized heating nature of the laser beam, huge thermal gradients exist across the melt pool and into the substrate. The thermal history of melt pool determines the microstructure of material and thus mechanical properties of resulting parts. Melt pool peak temperature and dimension are two essential parameters to characterize its thermal behavior and control of them is essential in obtaining consistent building performance in the laser metal deposition process, such as geometrical accuracy, microstructure, and residual stress [3]. On the other hand, these two variables are determined by the process parameters such as laser power, powder mass flow rate and scanning speed. So sensitivity analysis of the melt pool peak temperature and dimension to process parameters is of special interest.

Han et al. [4] numerically investigated the effects of process parameters on melt pool peak temperature and melt pool length, using the one-factor-at-a-time approach. This method consists of selecting a baseline set of levels for each factor, then successfully varying each factor over its range with the other factors held constant at the baseline set. The major disadvantage of this strategy is that it fails to consider any possible interaction between the factors.

Design of experiments (DOE) is a strong tool in sensitivity analysis for a manufacturing process. Typical design methods include factorial design, fractional factorial design, screening design,

response surface design and mixture design [5]. The most frequently used method is a factorial experiment, in which factors are varied together, instead of one at a time. One feature of this experimental strategy is that it makes the most efficient use of the experimental data. In the present work, a factorial design is applied to both the experiments and the simulations. This paper applies a joint experimental and numerical methodology to study the sensitivity of the melt pool peak temperature and length to process parameters variation.

## 2. Experimental study

### 2.1 Description of Experimental Set-up

Experiments were performed with the Laser Aided Material Processing system (LAMP) in the UMR-LAMP lab which consists of a 2.5-kw Nd:YAG laser, powder delivery unit, 5-axis CNC machine, and monitoring subsystem. Detailed description of the system was given by Liou et al. [6] and Boddu et al. [7]. A schematic of the system arrangement is shown in Fig. 1. The process output parameters (melt pool length, width and temperature) are monitored during deposition, along with process input parameters (laser power, scanning speed, and powder mass flow rate) and other process parameters (CNC axis position and velocity, powder feeder motor velocity). Melt pool temperature is monitored in real time using a dual-wavelength non-contact temperature sensor, which can effectively decrease the disturbance from the powder and other dusts. An axially mounted CMOS camera is used to take images of melt pool online during deposition. Melt pool dimensions are extracted using an image processing algorithm and are sent to the real time system [8]. Stainless steel 304 was chosen as the material for the substrate and powder.

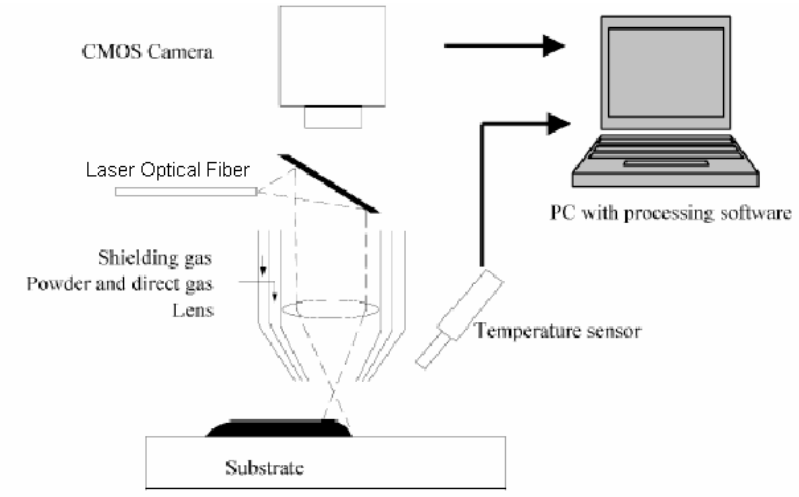


Fig. 1. Experimental setup

Other experimental set-up is as follows. Inner gas (powder direct gas) is 4.0 psi and outer gas (shielding gas) is 8.0 psi. The standoff distance is 0.35 inch. A 125 mm focusing lens was used to form a 0.7 mm (in diameter) spot. Inner gas is primarily used for protecting the laser focusing lens from stress due to reflection from the substrate. Outer gas shapes the powder stream onto the work piece. The standoff distance chosen above is such that the laser beam is focused on the work piece. The above parameters are held at these values for all experiments such that these settings do not affect the metal deposition process.

## 2.2 Design of Experiments

The major steps of implementing design of experiments are: (1) to identify the factors, (2) to identify the responses, (3) to identify the levels of each factor, (4) to conduct the experiments, (5) to analyze the experimental data, (6) and to conduct the confirmation experiment.

A two-level factorial design was used in this study. The design factors and levels are shown in Table 1. The held-constant factors include inner gas, outer gas, standoff distance and spot size as described in "2.1 Description of Experimental Set-up**"**. These design factors chosen are believed to be the most influential on the process. The responses under study are melt pool peak temperature and length.

Table 1. Factors and Levels

| Symbols and Factors | | Levels | |
|---|---|---|---|
| | | -1(Low Level) | +1 (High Level) |
| A | Laser power (W) | 500 | 800 |
| B | Powder mass flow rate (g/min) | 4 | 12 |
| C | Scanning speed (inch/min) | 10 | 25 |

## 2.3 Experimental layout and data

The experimental layout and data are shown in Table 2. Each run was conducted with two replicates. Due to the uncertainty of the powder injection location and the time interval between two consecutive particles, the melt pool peak temperature and length fluctuate throughout the process [4]. The average values during a certain period were taken as observations.

Table 2. Experimental layout and data

| Run | Coded Factors | | | Melt Pool Peak Temperature (K) | | Melt Pool Length (mm) | |
|---|---|---|---|---|---|---|---|
| | A | B | C | Replicate 1 | Replicate 2 | Replicate 1 | Replicate 2 |
| 1 | -1 | -1 | -1 | 2130.47 | 2154.79 | 1.09 | 1.03 |
| 2 | -1 | -1 | +1 | 1999.37 | 1997.02 | 0.87 | 0.99 |
| 3 | -1 | +1 | -1 | 1994.89 | 1970.53 | 0.86 | 0.70 |
| 4 | -1 | +1 | +1 | 1828.03 | 1832.35 | 0.66 | 0.64 |
| 5 | +1 | -1 | -1 | 2512.45 | 2492.12 | 1.66 | 1.76 |
| 6 | +1 | -1 | +1 | 2313.07 | 2331.37 | 1.53 | 1.73 |
| 7 | +1 | +1 | -1 | 2285.73 | 2240.03 | 1.61 | 1.59 |
| 8 | +1 | +1 | +1 | 2067.61 | 2111.37 | 1.49 | 1.53 |

## 2.4 Model Adequacy Checking

Before the analysis of variance is made, the adequacy of the underlying model should be checked. That is, we should avoid potential problems with the normality assumption and unequal error variance by treatment. The primary diagnostic tool is residual analysis.

The MINITAB® Release 14 software was used to check the model adequacy and to analyze the

factorial design. This is a general-purpose statistical software package with good data analysis capabilities.

Fig. 2 and Fig. 3 are the residual plots for melt pool peak temperature and length, respectively. It can be seen that for both melt pool peak temperature and length, none of the four types of residual plot reveals anything particularly troublesome, so we accept these responses as legitimate.

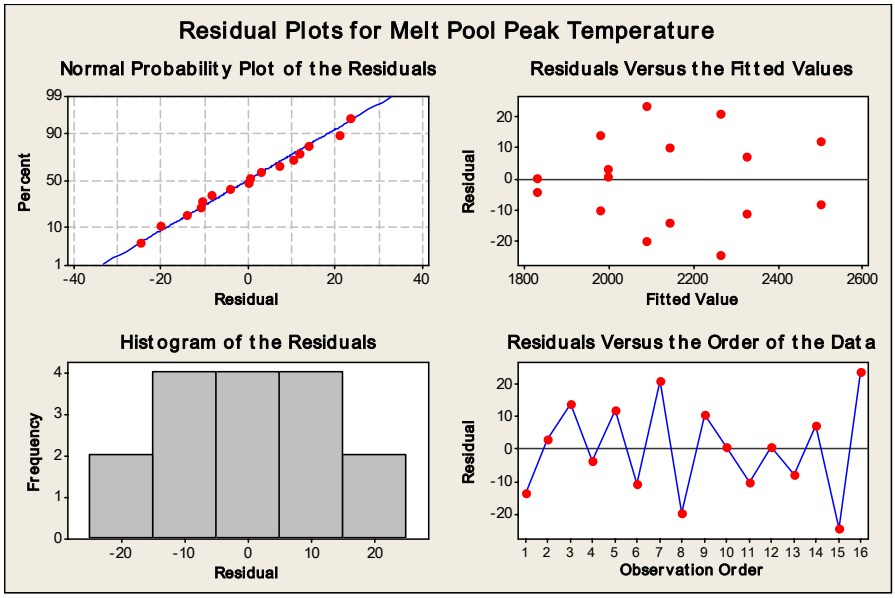


Fig. 2. Residual plots for melt pool peak temperature

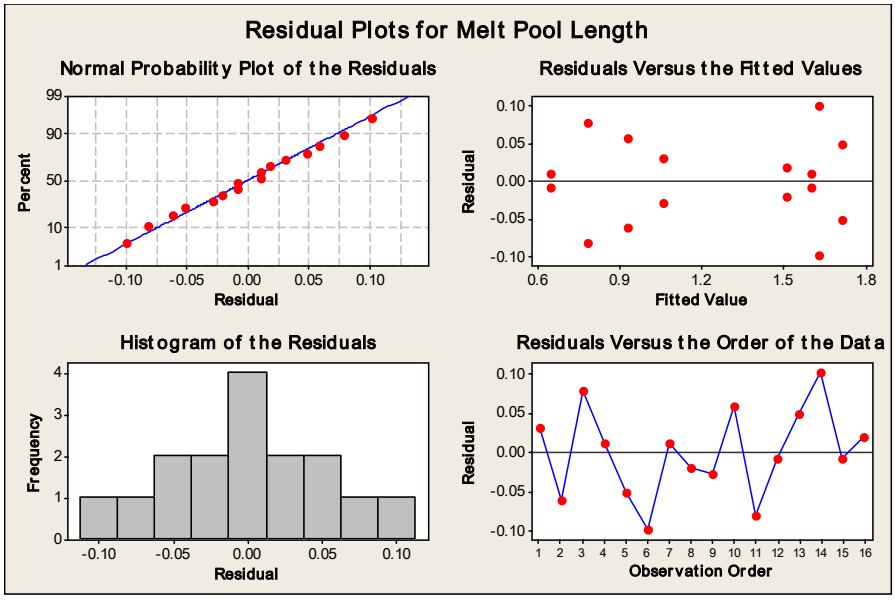


Fig. 3. Residual plots for melt pool length

## 2.5 Analysis of Data

2.5.1 Analysis of Variance

Table 3 and Table 4 summarize the effect estimates, sums of squares, percent contribution and P-values from the analysis of variance for the melt pool peak temperature data and for the melt pool length data, respectively. The percent contribution is a rough but effective guide to the relative importance of each model term [9]. P-value is the smallest level of significance at which the data are significant. P-value approach is adopted widely in practice, because it makes it possible for a decision maker to draw a conclusion at any specified level of significance. Table 3 and Table 4 indicate that for both melt pool peak temperature and length, the main effects really dominate, accounting for over 99 and 98 percent of the total variability, respectively. For both melt pool peak temperature and length, the AB interaction is significant, indicating that there is interaction between laser power and powder mass flow rate, and all the other interaction effects are not significant.

Table 3. Effect Estimate Summary for Melt Pool Peak Temperature

| Model Term | Effect Estimate | Sum of Squares | Percent Contribution | P-Value |
|---|---|---|---|---|
| A | 305.785 | 374017.86 | 57.7874 | 0.000 |
| B | -200.015 | 160024.00 | 24.7244 | 0.000 |
| C | -162.6 | 105755.04 | 16.3396 | 0.000 |
| AB | -36.05 | 5198.41 | 0.8032 | 0.006 |
| AC | -14.125 | 798.06 | 0.1233 | 0.181 |
| BC | -0.355 | 0.50 | 7.73E-05 | 0.972 |
| ABC | 3.69 | 54.46 | 0.0084 | 0.712 |
| Pure error | | 1382.781 | 0.2136 | |
| Total | | 647231.11 | | |

Table 4. Effect Estimate Summary for Melt Pool Length

| Model Term | Effect Estimate | Sum of Squares | Percent Contribution | P-Value |
|---|---|---|---|---|
| A | 0.7575 | 2.295225 | 90.6639 | 0.000 |
| B | -0.1975 | 0.156025 | 6.1632 | 0.001 |
| C | -0.1075 | 0.046225 | 1.8259 | 0.024 |
| AB | 0.0825 | 0.027225 | 1.0754 | 0.066 |
| AC | 0.0225 | 0.002025 | 0.0800 | 0.577 |
| BC | -0.0025 | 0.000025 | 0.0010 | 0.950 |
| ABC | -0.0025 | 0.000025 | 0.0010 | 0.950 |
| Pure error | | 0.0048 | 0.1896 | |
| Total | | 2.5316 | | |

2.5.2 The Regression Models and Response Surfaces

After the analysis of variance, it is a logic step to develop an interpolation equation for the response variables in the experiment. When one or more of the factors in the experiment are quantitative, regression models are particularly useful [9]. The level of significance is set at 0.05. The regression models for predicting melt pool peak temperature and length are:

$$\hat{y}_1 = \beta_0 + \beta_1 x_1 + \beta_2 x_2 + \beta_3 x_3 + \beta_{12} x_1 x_2$$

$$= 2141.325 + 152.8925 x_1 - 100.0075 x_2 - 81.3 x_3 - 18.025 x_1 x_2 \quad (1)$$

$$\hat{y}_2 = \beta_0 + \beta_1 x_1 + \beta_2 x_2 + \beta_3 x_3 + \beta_{12} x_1 x_2$$

$$= 1.23375 + 0.37875 x_1 - 0.09875 x_2 - 0.05375 x_3 + 0.04125 x_1 x_2 \qquad (2)$$

where $\hat{y}_1$ and $\hat{y}_2$ are melt pool peak temperature and length, respectively. The coded variable $x_1$, $x_2$, and $x_3$ represent A, B, and C, respectively. The $x_1x_2$ term is the AB interaction.

Fig. 4 and Fig. 5 present the response surfaces and contour plots for melt pool peak temperature and length obtained from the regression models, respectively, assuming that scanning speed is at the high level ($x_3 = 1$).

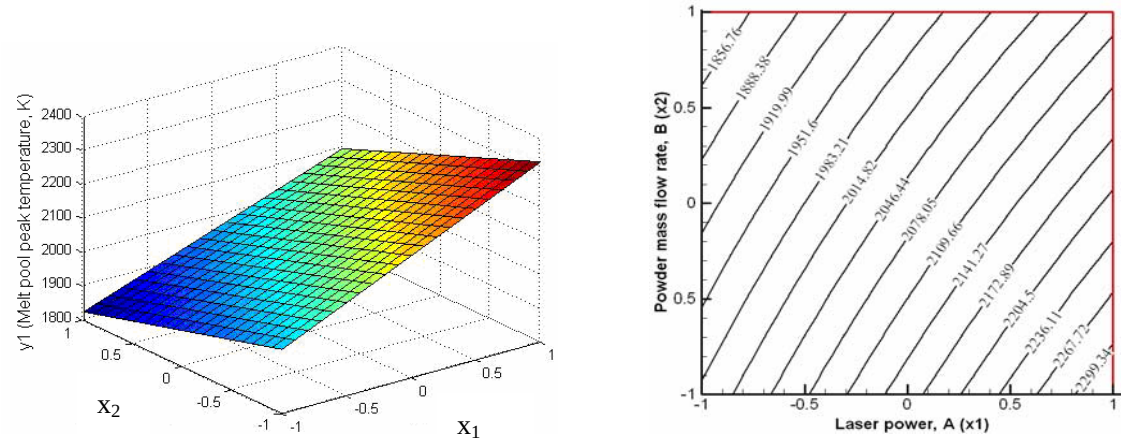


(a) The response surface (b) The contour plot

Fig. 4. Response surface and contour plot of melt pool peak temperature with scanning speed at the high level (25 ipm)

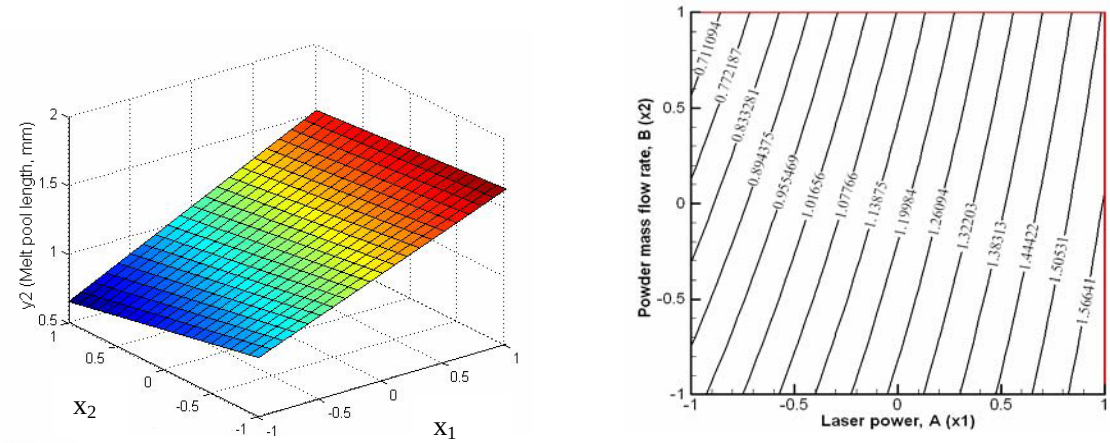


(a) The response surface (b) The contour plot

Fig. 5. Response surface and contour plot of melt pool length with scanning speed at the high level (25 ipm)

2.5.3 Confidence Interval on the effects

A confidence interval shows a range within which the value of the parameter or parameters in question would be expected to lie. Confidence intervals are preferable to p-values, as they tell us the

range of possible parameter sizes compatible with the data. The standard deviations of the effects can be obtained from the above analysis of variance:

SE (effect) = 4.825 (for melt pool peak temperature)

SE (effect) = 0.01936 (for melt pool peak length)

The residual degrees of freedom is DF = 8. If the level of significance, $\alpha = 0.05$, the t-percentile is $t_{\alpha/2, DF} = t_{0.025, 8} = 2.306$. Confidence intervals can be obtained by multiplying the t-percentile with the residual degrees of freedom. Approximate 95 percent confidence intervals on the factor effects are shown in Table 5.

Table 5. Confidence intervals on the factor effects

| Model Term | Confidence Interval on the Factor Effects | |
|---|---|---|
| | Melt Pool Peak Temperature (K) | Melt Pool Length (mm) |
| A | 305.785 ± 11.1265 | 0.7575 ± 0.0446 |
| B | -200.015 ± 11.1265 | -0.1975 ± 0.0446 |
| C | -162.6 ± 11.1265 | -0.1075 ± 0.0446 |
| AB | -36.05 ± 11.1265 | 0.0825 ± 0.0446 |
| AC | -14.125 ± 11.1265 | 0.0225 ± 0.0446 |
| BC | -0.355 ± 11.1265 | -0.0025 ± 0.0446 |
| ABC | 3.69 ± 11.1265 | -0.0025 ± 0.0446 |

This analysis indicates that for melt pool peak temperature, A, B, C, AB, and AC are important factors, and for melt pool length, A, B, C, and AB are important factors, because they are the only factor effect estimates for which the approximate 95 percent confidence intervals do not include zero.

## 3. Numerical Simulations

### 3.1 Modeling of the laser deposition process

3.1.1 Introduction to the model

The present simulation work builds directly on modeling and simulation work by Han et al. [4] and hence some details of the model and simulation will be omitted. This model considers most phenomena occurring in the laser deposition process, such as melting, solidification, evaporation, evolution of melt pool surface and powder injection. Besides the fluid flow in the melt pool and the energy balance at the liquid-vapor and the solid-liquid interfaces, laser power attenuation due to the powder cloud is incorporated into the model. The evolution of the free surface is tracked with the level set method. Simulation is based on the semi-implicit finite difference method.

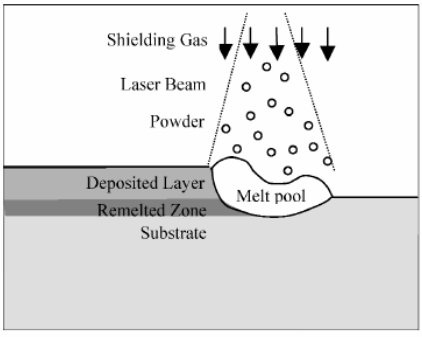


Fig. 6. Schematic of the calculation domain for the laser deposition

3.1.2 Main governing equations

The calculation domain, illustrated in Fig. 6, includes the substrate, deposited layer, re-melted zone,

melt pool, and part of the gas region. The continuum model [10, 11], which introduce the Darcian damping term, is applied to the mushy region, liquid region and solid region, and it can be expressed as the following equations. The governing equation for mass conservation is given by:

$$\frac{\partial \rho}{\partial t} + \nabla \cdot (\rho \vec{V}) = 0 \tag{3}$$

The governing equations for momentum conservation are given by:

$$\frac{\partial}{\partial t}(\rho u) + \nabla \cdot (\rho \vec{V} u) = \nabla \cdot (\mu_l \frac{\rho}{\rho_l} \nabla u) - \frac{\partial p}{\partial x} - \frac{\mu_l}{K} \frac{\rho}{\rho_l}(u - u_s) + S_{\phi x} \tag{4}$$

$$\frac{\partial}{\partial t}(\rho v) + \nabla \cdot (\rho \vec{V} v) = \nabla \cdot (\mu_l \frac{\rho}{\rho_l} \nabla v) - \frac{\partial p}{\partial y} - \frac{\mu_l}{K} \frac{\rho}{\rho_l}(v - v_s) + \rho g + S_{\phi y} \tag{5}$$

The governing equation for energy conservation is given by:

$$\frac{\partial (\rho h)}{\partial t} + \nabla \cdot (\rho \vec{V} h) = \nabla \cdot (k \nabla T) - \nabla \cdot (\rho (h_l - h)(\vec{V} - \vec{V}_s) \tag{6}$$

where ρ is density, t is time, $\vec{V}$ is velocity vector, u and v are velocity components in x and y direction, respectively, μ is dynamic viscosity, K is permeability of the two-phase mushy zone, $S_{\phi x}$ and $S_{\phi x}$ are source terms contributed by the interfacial forces, p is pressure, g is gravity acceleration, h is enthalpy, k is thermal conductivity, subscripts l and s represents liquid and solid, respectively.

The evolution of the melt pool free surface is tracked with the level set method [12, 13]. The evolution equation of the melt pool free surface is given by:

$$\frac{\partial \phi}{\partial t} + F |\nabla \phi| = 0 \tag{7}$$

where ϕ is a distance function, F is a speed function, which is dependent on interfacial forces such as surface tension, thermo-capillary force, and vapor pressure.
In the preceding governing equations, mixture properties are used for density, specific heat, conductivity, enthalpy and velocity vector by using mass or volume fractions of solid and liquid phases.

3.1.3 Initial and Boundary Conditions

Initially, the calculation domain is assumed not to contain liquid material and to have the ambient temperature uniformly. Other variables, including velocities and pressure, are equal to zero. The rigid free-slip wall conditions are imposed on all the four mesh boundaries so that the normal velocities are zero.

### 3.3 Simulation Results and Statistical Analysis

Numerical simulations were conducted according to the design of experiments. The results are shown in Table 6. Although these results are not experimental data, we can use DOE method to analyze them. The purpose is to compare these statistical analysis results with the analysis results for the experimental data. Table 7 and Table 8 summarize the effect estimates, sums of squares and

percent contribution from the analysis of variance for the simulated melt pool peak temperature and length, respectively.

Table 6. Simulation layout and results

| Run | Coded Factors | | | Melt Pool Peak Temperature (K) | Melt Pool Length (mm) |
|---|---|---|---|---|---|
| | A | B | C | | |
| 1 | -1 | -1 | -1 | 2259.74 | 0.88 |
| 2 | -1 | -1 | +1 | 2107.34 | 0.80 |
| 3 | -1 | +1 | -1 | 2144.23 | 0.62 |
| 4 | -1 | +1 | +1 | 1915.56 | 0.56 |
| 5 | +1 | -1 | -1 | 2607.54 | 1.57 |
| 6 | +1 | -1 | +1 | 2479.36 | 1.54 |
| 7 | +1 | +1 | -1 | 2373.71 | 1.42 |
| 8 | +1 | +1 | +1 | 2217.58 | 1.25 |

Table 7. Effect Estimate Summary for Simulated Melt Pool Peak Temperature

| Model Term | Effect Estimate | Sum of Squares | Percent Contribution |
|---|---|---|---|
| A | 312.84 | 195737.7 | 57.7559 |
| B | -200.72 | 80577.04 | 23.7757 |
| C | -166.34 | 55337.99 | 16.3285 |
| AB | -47.08 | 4433.053 | 1.3081 |
| AC | 24.18 | 1169.345 | 0.3450 |
| BC | -26.06 | 1358.247 | 0.4008 |
| ABC | 12.08 | 291.8528 | 0.0861 |
| Total | | 338905.3 | |

Table 8. Effect Estimate Summary for Simulated Melt Pool Length

| Model Term | Effect Estimate | Sum of Squares | Percent Contribution |
|---|---|---|---|
| A | 0.73 | 1.0658 | 89.0690 |
| B | -0.235 | 0.11045 | 9.2303 |
| C | -0.085 | 0.01445 | 1.2076 |
| AB | 0.015 | 0.00045 | 0.0376 |
| AC | -0.015 | 0.00045 | 0.0376 |
| BC | -0.03 | 0.0018 | 0.1504 |
| ABC | -0.04 | 0.0032 | 0.2674 |
| Total | | 1.0784 | |

### 3.4 Comparisons between numerical and experimental results

Melt pool peak temperature and length comparisons between simulation and experiments are shown in Fig. 7 and Fig. 8. It can be seen that the simulation results agree well with experimental data, although there is about 120 K over-prediction on average in peak temperature, and about 0.15 mm under-prediction on average in melt pool length.

For the effect estimate and percent contribution of each model term, the general trend between simulation and experiments is consistent. That is, the main effects dominate in the process, and factor A (laser power) really governs the melt pool length.

There are also some disagreements between experiments and simulation. Note that for both melt pool peak temperature and length, the AC interaction effect has different signs for simulation and experiments. Fortunately, this interaction effect is not significant. One possible explanation for these disagreements is the over-prediction or under-prediction of simulations, the reason of which will be explored in the next section.

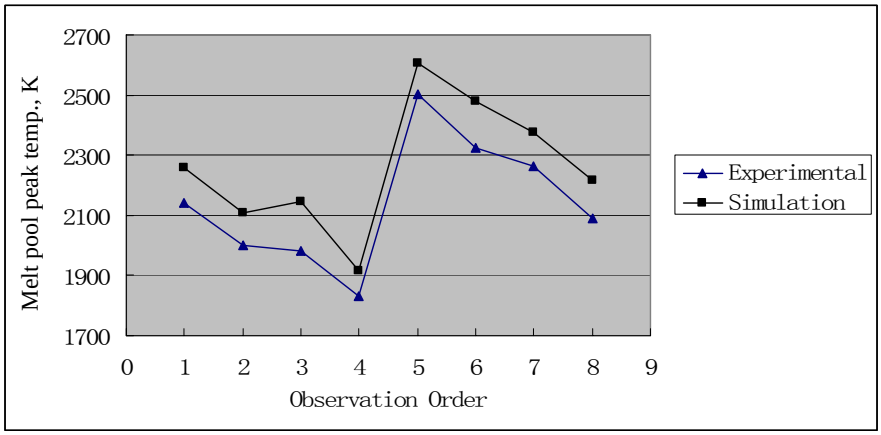


Fig. 7. Melt pool peak temperature comparisons between simulation and experiments

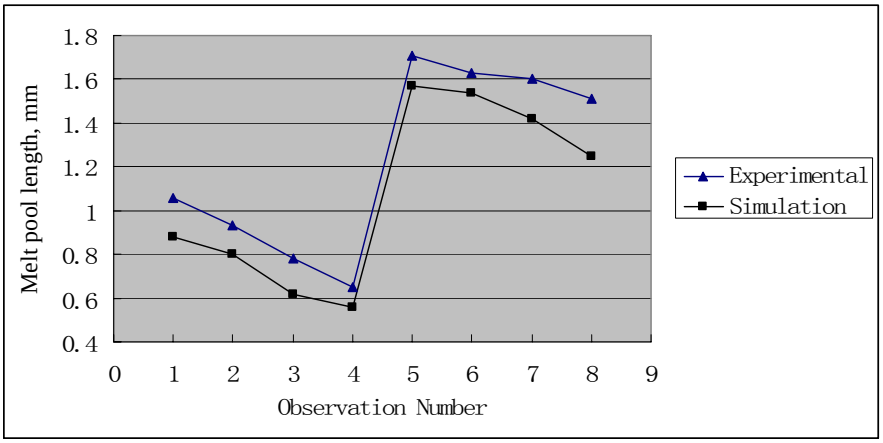


Fig. 8. Melt pool length comparisons between simulation and experiments

## 4. Discussion

The present work is a quantitative investigation on the effects of process parameters on melt pool thermal behavior. Qualitative description of the effects can be found in literature (for example, [4]), which is reiterated here. An increase in laser power increases the melt pool temperature and dimension. An increase in scanning speed decreases the melt pool temperature and length, since the increase of scanning speed reduces the laser material interaction time. An increase in powder mass flow rate decreases the melt pool temperature and length, which can be explained by laser power attenuation due to the powder cloud. As the powder mass flow rate increases, the amount of energy

required for melting the powder increases and thus the amount of laser power for melting the substrate decreases.

The disagreements between experiments and simulation may arise from the following main sources: (1) Alteration of the material properties at different temperatures, which were regarded as constants in the simulation. (2) Discrepancies between the values adopted in the simulation and the real values of the following efficiency coefficients: the laser-energy-transfer efficiency, which represents the fraction of laser output energy that is actually absorbed by the workpiece; the melting efficiency, which represents the fraction of absorbed energy which is utilized for melting; deposition efficiency, which is defined as the ratio of the actual deposition rate (i.e., the rate of powder actually incorporated into the melt pool) to the set powder mass flow rate [14]. (3) Irregularity of the powder particles, which were treated as spheres in the simulation.

From the statistical analysis of experimental data, it can be seen that laser power and powder mass flow rate have an interaction effect on both melt pool peak temperature and length. This interaction effect is negative for melt pool temperature but positive for melt pool length. A possible explanation is that laser power governs the melt pool size but its effect for melt pool temperature is at the same level as those of powder mass flow rate and scanning speed, although the former is apparently greater than the latter. So for melt pool length, laser power attenuation effect at higher laser power level is not as significant as at lower laser power.

## 5. Conclusions and further work

This paper experimentally and numerically analyzed the sensitivity of process parameters in laser deposition, using a factorial design. The significant factors and their interactions were determined through statistical analysis of the results. The regression models for predicting melt pool peak temperature and length have been built.

The simulation results were compared to experimental results and good quantitative agreement was found although there were some disagreements. The physical interpretation of the results was made. This quantitative sensitivity analysis of process parameter can be a guide for the control of melt pool thermal behavior and thus building performance in the laser deposition process.

Based on the results obtained in the present study, the following main conclusions can be drawn:

1) The main effects dominate in the process.
2) There is an interaction effect between laser power and powder mass flow rate.
3) Laser powder, powder mass flow rate and scanning speed are the first, second and third most influential factor, respectively. And laser power really governs the melt pool length.
4) The numerical simulation can reliably predict melt pool thermal behavior in the laser deposition process.

The following work can be considered as further research on the effects of process parameters on melt pool thermal behavior:

1) To include other process parameters in the design factors, for example, shielding gas, standoff distance, spot size and laser mode.

2) To use a central composite design or response surface method to conduct experiments. Thus more factor levels are needed but second-order or quadratic factor effects can be checked.

## ACKNOWLEDGEMENTS

This research was supported by the National Science Foundation Grant Number DMI-9871185, Army Research Office, and Air Force Research Laboratory and UMR Intelligent Systems Center. Their support is appreciated.

## References

1. Robert G. Landers, Fourteenth Annual Solid Freeform Fabrication Symposium, Austin, Texas, August 4–6, 2003, pp.246-253.
2. Vinay Kadekar, Sashikanth Prakash and Frank Liou, Fifteenth Annual Solid Freeform Fabrication Symposium, Austin, Texas, 2004, pp.198-202.
3. Lijun Han, Frank W. Liou and Srinnivas Musti, PhD thesis, University of Missouri-Rolla, 2005.
4. L. Han, F.W. Liou and K.M. Phatak, Metall. Mater. Trans. B, Vol. 35B, No. 6, pp. 1139-1150B, Dec. 2004.
5. H. M. Wadsworth, Handbook of Statistical Methods for Engineers and Scientists, McGraw-Hill, Inc., 2nd ed., 1998.
6. F. Liou, J. Choi, R. Landers, V. Janardhan, S. Balakrishnan, and S. Agarwal, Proc. 12th Annual Solid Freeform Fabrication Symp., Austin, TX, Aug. 6–8, 2001, pp. 138-45.
7. M. Boddu, S. Musti, R. Landers, S. Agarwal, and F. Liou, Proc. 12th Annual Solid Freeform Fabrication Symp., Austin, TX, Aug. 6–8, 2001, pp. 452-59.
8. Kaushik Phatak, Master thesis, University of Missouri-Rolla, 2005.
9. Douglas C. Montgmetry, Design and analysis of experiments, New York : John Wiley, 5th ed., 2001
10. W. Bennon and F. Incropera, Int. J. Heat Mass Transfer, 1987, vol. 30, pp. 2161-70.
11. W. Bennon and F. Incropera, Int. J. Heat Mass Transfer, 1987, vol. 30, pp. 2171-87.
12. J.A. Sethian, Level Set Methods and Fast Marching Methods, 2nd ed., Cambridge University Press, Cambridge, United Kingdom, 1999.
13. M. Sussman, P. Smereka, and S. Osher, J. Comp. Phys., 1994, vol. 114, pp. 146-59.
14. R.R. Unocic and J.N. DuPont, Metall. Mater. Trans. B, Vol. 34B, No.4, pp. 439-445, Aug. 2003.